




Myocardial perfusion imaging using single-photon emission computed tomography with cadmium-zinc-telluride technology: a review

Sonia J. Konsek-Komorowska¹, Mariola Peczkowska², Jaroslaw B. Cwikla^{1,3}

¹Department of Cardiology and Internal Medicine, School of Medicine, Collegium Medicum, University of Warmia and Mazury in Olsztyn, Olsztyn, Poland

²Department of Hypertension, The Cardinal Stefan Wyszyński National Institute of Cardiology, Warsaw, Poland

³Diagnostic and Therapeutic Center — Gammed, Warsaw, Poland

[Received 21 I 2022; Accepted 9 VI 2022]

Abstract

Myocardial perfusion imaging (MPI) with single-photon emission computed tomography (SPECT) is a well-established diagnostic approach for patients with suspected or confirmed coronary artery disease (CAD). In the present century, nuclear cardiology has benefited immensely from advances in imaging instrumentation and technology. Dedicated cardiac SPECT cameras incorporating novel, highly efficient cadmium-zinc-telluride (CZT) detectors, collimators, and system designs have evolved as a result of the expansion of nuclear cardiology. A vast amount of evidence is emerging, demonstrating the new technology's advantages over the traditional gamma cameras. Myocardial perfusion imaging (MPI) using gamma-cameras with CZT detectors may be performed with the limited injected activity of radiotracer and recorded times. The use of CZT's dynamic acquisition of myocardial perfusion imaging in clinical practice may help cardiologists in detecting hemodynamically significant CAD. In this article, we present the current state of knowledge on cardiac CZT-SPECT scanners, a summary of the literature published on validation studies, radiation dose reduction, and dynamic acquisition, as well as a comparison of conventional myocardial perfusion imaging with invasive coronary angiography.

KEY words: myocardial perfusion imaging; CZT; coronary artery disease; CAD; cadmium-zinc-telluride single-photon emission computed tomography; CZT-SPECT; CZT; nuclear cardiology

Nucl Med Rev 2022; 25, 2: xx–xx

Introduction

Myocardial perfusion imaging (MPI) is a useful approach for identifying coronary artery disease (CAD) which is a pathological condition defined by atherosclerotic plaque formation in the epicardial arteries, and can be obstructive or non-obstructive [1]. Functional non-invasive test such as single-photon emission

computed tomography (SPECT) for the diagnosis of obstructive CAD is designed to detect perfusion changes. Exercise or pharmacological stressors can cause ischemia by increasing cardiac work and oxygen requirement or by heterogeneity in myocardial perfusion caused by the widening of blood vessels [2]. Invasive coronary angiography (CAG) has been the gold standard in the diagnosis of CAD for many years. However, one of the major drawbacks of this approach is that it only gives anatomical evaluation. MPI is superior to anatomical evaluation alone in terms of providing information regarding myocardial viability and function [3, 4]. When compared to invasive functional testing fractional flow reserve (FFR), non-invasive functional tests are linked with high accuracy in the diagnosis of flow-limiting coronary stenosis. According to the European Society of Cardiology Guidelines for the diagnosis and

Correspondence to: Sonia J. Konsek-Komorowska
 Department of Cardiology and Internal Medicine, School of Medicine,
 Collegium Medicum, University of Warmia and Mazury in Olsztyn,
 Warszawska 30, 10-082 Olsztyn, Poland
 phone: +48 89 524 53 89
 e-mail: sonia.konsek@interia.pl

management of chronic coronary syndromes from 2019, non-invasive functional imaging for myocardial ischemia such as SPECT or coronary computed tomography angiography (CTA) is indicated as the initial test for identifying CAD in symptomatic individuals in whom clinical examination alone cannot rule out obstructive CAD. Myocardial perfusion imaging (MPI) with SPECT may be used in conjunction with dynamic exercise testing and can be chosen if extra information from the exercise test, for example, heart rate response to activity or exercise tolerance, is deemed significant [2]. MPI use has increased significantly over the last decade, and it is currently the most widely utilized non-invasive imaging method for risk stratification in patients with suspected or known CAD [5].

Nowadays, there is a trend for identifying strategies and protocols to minimize radiation exposure for patients as well as for standard laboratory operating procedures. Weighing the dosimetry of currently used cardiac imaging procedures would be a first step toward implementing a test choice technique to reduce overall risk to individuals while retaining excellent diagnostic data [6]. From a clinical standpoint, a few important matters should be well-thought-out when approaching diagnostic imaging: the first is the need to take close notice of the issue of radiation exposure and associated hazards, and the second is the recognition that imaging techniques must demonstrate a solid ability to affect patient supervision by enhancing clinical outcomes. This attention points to the selection of a lower-radiation-dose imaging modality among those available, based on the clinical benefit for a specific patient.

Several attempts to enhance the MPI approach through the use of iterative reconstruction algorithms [7, 8], early-imaging protocols [9], or new tracers [10] yielded excellent discoveries but no breakthroughs that turned into applications that improved everyday clinical practice [4]. New low-dose procedures and new technology have been developed to address these issues, expanding the use of MPI in clinical practice [1]. Detectors based on cadmium zinc telluride (CZT) have been used in SPECT imaging systems since the first decade of the 21st century [11, 12]. When compared to typical gamma cameras, myocardial perfusion scintigraphy may be conducted more quickly and with less radiation exposure [3, 11]. These devices have more sensitive solid-state CZT detectors and have greater spatial and energy resolution than the conventional type of camera which employs the use of a scintillation detector, applying sodium iodide crystal activated by thallium (NaI [Tl]) [11, 12].

In this review article, we aim to present a detailed description of the diagnostic value of CZT-SPECT and a number of technical points associated with image acquisition, data post-processing, and as well as interpretation. A brief summary of prior accomplished investigations with CZT-SPECT cameras is also given.

Cadmium-zinc-telluride SPECT scanners

The CZT detector functions as a semiconductor, converting gamma radiation directly to an electric signal. This mechanism improves spatial resolution and sensitivity, resulting in a lower given dose of radiopharmaceuticals and/or a quicker acquisition time [12]. There are now two commercially available CZT-SPECT scanners: D-SPECT (Spectrum Dynamics, Caesarea, Israel) and Discovery 530 or Discovery 570c (GE Healthcare, Waukesha, WI, USA) [11]. Both systems employ solid-state CZT detector assemblies, which are made up of smaller units that individually produce

projection data in a 16×16 matrix with 2.46×2.46 mm pixels. The cadmium zinc telluride thickness is 5 mm, and both scanners utilize identical CZT modules. Each pair producing current is separated by the voltage across the crystal. There is no scintillation and no photomultipliers, unlike traditional Anger cameras [13]. D-SPECT, which employs pixelated cadmium zinc telluride detector arrays in nine vertical columns arranged in a 90° gantry geometry, is one of the most often used systems. Tungsten is used to make the parallel hole high sensitivity collimators. Discovery 530 or Discovery 570c model is built on a multi-pinhole collimator system and a pixelated array of 19 cadmium zinc telluride detectors [12]. Image quality has improved in both systems due to increased sensitivity in detecting cardiac activity [1]. The spatial resolution of the GE Discovery was stated to be superior (6.7 mm) compared to D-SPECT (8.6 mm). On the contrary, the count sensitivity of the D-SPECT was reported to be higher (850 counts per second per MBq) compared to GE Discovery (460 counts per second per MBq). Those two parameters outperform the standard SPECT mean values (15.3 mm of spatial resolution and sensitivity of 130 counts per second per MBq) [12, 14]. These results show a significant improvement in image quality, owing to a decreased amount of Compton photons inside the acquisition energy window [1]. D-SPECT and GE Discovery use iterative reconstruction, but with different filters as well as reconstruction parameters, such as the number of iterations and subsets employed [11]. The creation of a specific three-dimensional iterative reconstruction technique based on maximum likelihood expectation maximization, which adjusted for the loss in spatial resolution caused by the collimator's line response function, enhanced CZT picture quality even more [15].

Clinical validation tests revealed that the innovative CZT camera allowed for a more than five-fold decrease in scan duration while providing clinical information comparable to typical SPECT MPI [16, 17]. In the first study comparing ultrafast versus traditional cameras for detecting obstructive coronary artery disease, using CAG as the gold standard, the CZT scanner detected a greater number of vessels with obstructive CAD, regardless of comparable diagnostic confidence on a per-patient basis [18]. According to these findings, an ultrafast device provides a more precise assessment of the extent and severity of myocardial ischemia in individuals with coronary artery disease [19]. Accordingly, the greatest improvement has been recorded in the left circumflex (LCX) and right coronary artery (RCA) territories, resulting in a clearer demarcation of multi-vessel CAD and highlighting the tremendous relevance for therapeutic application in subjects with severe coronary artery disease, as verified by many investigations [16–18].

Radiation dose reduction

The possibility of carcinogenesis from radiation connected with medical imaging examinations is still being debated in the literature. The radiation linked with SPECT MPI comes from a gamma-emitting isotope administered intravenously usually in two doses. The majority of patients showed no genotoxic effects following SPECT MPI, but a minority (about one-third) exhibited both protein phosphorylation and elevated expression of DNA damage genes, indicating a heightened vulnerability to radiation effects [20]. In addition, it became clear that it is extremely challenging to objectively show any impairment that low doses of radiation can possibly cause on patients [1].

Radiation dosage reduction is currently amongst the most common pitfalls in diagnostic procedures. Although nuclear medicine procedures are not the primary source of radiation exposure in medical management when compared to computed tomography, reducing provided dosages of radiopharmaceuticals is beneficial for both patients and nuclear cardiology personnel [12].

Preliminary reports [21] and early clinical studies [22, 23] demonstrated the possibility of reducing acquisition time for stress and rest myocardial perfusion imaging. Based on these initial findings, the device with efficient cadmium-zinc-telluride detectors rendered a significant milestone for the everyday use of myocardial perfusion imaging in clinical practice [1].

Duvall et al. [24] reported the clinical experience with a CZT scanner and dosage reduction. The authors retrospectively analyzed images of 717 patients, which were obtained using ^{99m}Tc -sestamibi stress gated SPECT MPI studies done on a CZT camera (Discovery NM 530c). The MPI procedures were carried out within a four-month period, and subjects were categorized into three groups depending on the protocol: low-dose stress-only, high-dose stress-only, and low-dose rest high-dose stress. The ^{99m}Tc stress dosage for the low-dose protocol was 462.5 MBq, whereas the high dose ranged from 925–1332 MBq depending on the patient's weight. The low-dose rest dose was 296–481 MBq which was likewise weight-adjusted. In comparison to the standard rest-stress doses, radiation activity was reduced by 70% in the low-dose stress-only group and 30% in the high-dose stress-only group. In comparison to standard rest-stress doses, the effective dose in the low-dose stress-only group was reduced by 64% on average and by 32% in the high-dose stress-only group. A comparable number of total counts were obtained after MPI for 5 minutes in low-dose stress-only subjects and 3 minutes in high-dose stress-only and rest-stress patients. The low-dose stress-only group had a 57% isotope dose reduction in comparison to the high-dose stress-only subjects, resulting in identical picture quality in all three groups [24].

In further research, compared to a scintillation camera, image quality or diagnostic accuracy were not affected by lowering acquisition time with a low administered dose. On the CZT camera, acquisition times were five and eight minutes for rest, three and five minutes for stress images, and fifteen minutes for stress on traditional SPECT. There was no significant difference between CZT and conventional cameras concerning ejection fraction (EF), mean perfusion deficit, or left ventricular (LV) volumes assessed by the acquisition time (short versus long). Despite the shorter time and lower total impulse count, the pictures acquired by CZT SPECT were of substantially higher quality [25].

According to a report by Einstein et al. [26] the picture quality, EF, and total perfusion deficit (TPD) acquired by the CZT device were all in satisfactory correlation using an ultra-low-dose protocol (with radiation exposure of about 1 mSv).

Diagnostic value of CZT-SPECT in coronary artery disease

The integrated technique, which combines cardiac imaging with gated SPECT to measure perfusion and function, has been proved to be beneficial in tissue characterization and prognosis, giving essential data for clinical management in subjects with suspected

or confirmed coronary artery disease [1]. The results of perfusion images acquired with the CZT-SPECT and Anger SPECT cameras were found to be very consistent. Esteves et al. [22] compared images acquired with the Discovery NM 530c and conventional gamma cameras in multicenter research involving 168 patients. The images had a 91.9% concordance in detecting or excluding ischemia in comparison to a 92.5% agreement when the same examinations performed with a conventional camera were reviewed twice, $p = 0.99$. Sharir et al. [27] revealed, in a multicenter analysis including 238 subjects, high agreement of quantitative evaluation of TPDs (linear correlation coefficients for D-SPECT and Anger SPECT in the stress and rest examinations equaled 0.95 and 0.97, respectively) with a strong concordance in areas supplied by three main vessels (kappa coefficients for the left anterior descending coronary artery (LAD) and left circumflex coronary artery (LCX) were 0.73, and for right coronary artery (RCA) was 0.70, the agreement in identifying ischemia in each of the three territories supplied by LAD, LCX and RCA exceeded 90%).

Cantoni et al. [28] revealed, in relation to CAG, that MPI using SPECT with CZT detectors is a beneficial tool that can be used appropriately in the identification of CAD in a meta-analysis of 40 studies involving a total of 7734 patient studies on the diagnostic efficacy of SPECT using CZT detectors and Anger SPECT. Its diagnostic efficacy was marginally higher than that of a conventional SPECT camera in comparison to CAG [sensitivity 89% versus 85%, specificity 69% versus 66%, areas under the ROC curve (AUC) 0.89 versus 0.83]. The accuracy of SPECT using CZT detectors studies was minimally, but statistically significant, greater than that of Anger SPECT examinations ($p = 0.05$). This may be explained by the increased contrast of images generated with semiconductor gamma cameras due to improved spatial resolution. Earlier meta-analyses concerning studies on semiconductor cameras combined with CAG conducted by Nudi et al. [29] on 2092 subjects and Zhang et al. [30] on 2350 subjects found comparable outcomes in terms of study sensitivity and specificity in the detection of CAD, with no significant alterations between the two CZT devices utilized in the study.

Gimelli et al. [31] demonstrated, using data from 695 individuals, that a CZT camera may identify coronary artery disease in subjects with multivessel disease. The AUCs determined using semi-quantitative measures — summed stress scores (SSS) — in patients with two- and three-vessel disease, 0.83 and 0.79, respectively, did not differ substantially from the area under the ROC curve in single-vessel patients — 0.80. In 64% of patients, this approach correctly detected the severity of CAD. Regional perfusion abnormalities associated with the location of the three main coronary arteries were recognized with high efficiency (AUC for LAD was 0.90, for LCX was 0.88, and for RCA was 0.87). The research by Gimelli et al. [31] reveals that semiconductor cameras outperform conventional cameras in terms of detecting patients with multivessel disease.

Attempts are undertaken to correct image attenuation to increase the quality of studies. According to Esteves et al. [32], attenuation correction of CZT SPECT images has no significant effect on their visual interpretation. Another method for improving study quality is to rotate the patient during data acquisition, expecting that the filling of perfusion deficits caused by a modification in subject position shows their incorrect origin. Only the Discovery

NM 530c camera allows for study acquisition in the prone and supine positions. In a meta-analysis of investigations employing conventional and semiconductor cameras, Mirshavalad et al. [33] revealed that the prone position study which included 1490 patients compared to the supine position study which included 1138 patients has similar sensitivity (83% versus 8%) and better specificity (79% versus 67%). The prone position has a pooled sensitivity and specificity of 70% and 84% in identifying right coronary artery territory defects, respectively. Nishiyama et al. [34] analyzed 276 subjects and indicated that using data from supine and prone position significantly enhances perfusion interpretation concerning specificity ($p = 0.02$) and accuracy ($p = 0.04$) when compared to the supine position: sensitivity, specificity, and accuracy were as follow: 85% versus 78%, 85% versus 50%, and 85% versus 76%, respectively. In the case of D-SPECT, studies may be obtained in the upright, supine, and biker-like positions. A study by Nakazato et al. [35] combined evaluation of images obtained in the upright and supine position, compared to the outcomes of invasive CAG, yielded a sensitivity of 94% and specificity of 86%, in comparison to examinations obtained only in the upright (91% and 59%) or only supine (88% and 73%) positions; AUCs varied statistically significantly (0.94 versus 0.88 and 0.89, $p < 0.05$). In comparison to the upright and supine positions, the forward-leaning biker-like position reduced the distance between the heart and the detector and removed attenuation artifacts [36].

Diagnostic value of CZT-SPECT in the assessment of left ventricular contractility

Various published data highlight the significance of CZT cameras for LV function evaluation, offering crucial data on the feasibility of using the new cameras for a combined assessment. Gated acquisition of an MPI with SPECT and a patient electrocardiogram signal (G-SPECT) improves the study's diagnostic usefulness by assessing regional and global LV contractility [37]. CZT-G-SPECT has been compared to gold standard magnetic resonance imaging (MRI) and Anger G-SPECT concerning LV functional parameters (end-systolic volume — ESV, end-diastolic volume — EDV, and EF) [38–40]. In studies on this topic, Cochet et al. [38], Giorgetti et al. [39], and Claudin et al. [40] found a high or moderately high correlation between the findings of EDV assessment (0.71; 0.90; 0.94, respectively) and ESV (0.88; 0.94; 0.96, respectively) in comparison to MRI [38–40]. Giorgetti et al. [39] found that reported volumes were greatly underestimated due to the lower resolution of CZT-SPECT cameras compared to MRI. Nonetheless, these changes had no significant impact on global EF evaluation. In general, strong correlations were found between the EF values acquired from G-SPECT using CZT detectors and MRI (0.81, 0.84, and 0.88, respectively) [38–40]. It is important to emphasize that because CZT cameras have a superior resolution, the values of LV volume estimates are less underestimated than with standard devices.

Sala et al. [41] compared LV volume and EF measurements using the Discovery device and MRI. Although the volume and EF were greatly correlated with magnetic resonance outcomes (EDV, ESV, and EF 0.91, 0.95, and 0.86, respectively), the ejection fraction was consistently significantly undervalued [48 (15%) versus 55 (18%); $p = 0.001$], while the ESV was consistently exaggerated [84 (71) versus 72 (63) mL; $p = 0.001$]. Alterations between findings and

what has been reported in those previous investigations are problematic to interpret.

The first clinical validation of MPI utilizing a CZT camera to assess regional and global left ventricular function shows outstanding concordance between cadmium-zinc-telluride technology and cardiac magnetic resonance (CMR). The low systematic bias (-2.7 percent) has been shown to have negligible clinical importance, and full wall thickening and wall motion estimates utilizing CZT devices may similarly be used to identify myocardial scarring, as determined by delayed enhancement in CMR. Myocardial perfusion imaging using CZT-SPECT scanners and quantitative gated SPECT analysis precisely quantifying the EF. However, in accordance with prior research comparing CMR and standard SPECT MPI, utilizing CZT cameras resulted in a considerable underestimate of ventricular volumes even with 16-frame gating [38].

According to research by Bailliez et al. [42] regional wall thickening was underestimated using CZT (Discovery 530 NMc) camera, particularly in individuals with higher wall thickness.

Coupez et al. [43] discovered the utility of segmental evaluation of LV myocardium thickening in the identification of post-infarction scarring, owing to a strong association of extreme deficiency of thickening found with the device with cadmium zinc telluride detectors and delayed post-contrast segment enhancement in magnetic resonance imaging.

Claudin et al. [40] found high concordance (kappa coefficient 0.72, strict agreement 87%) among the G-SPECT examination using the CZT device and the MRI when comparing LV contractility in 17 segments and assessed visually on a three-point scale: akinesis or dyskinesia, hypokinesia, and normal contractility.

The measurements of LV filling dynamics acquired using CZT camera correspond with echocardiographic diastolic function parameters obtained by echocardiography, boosting the sensitivity in detecting significant ischemic heart disease [44, 45].

Dynamic CZT-SPECT in coronary artery disease

Positron emission tomography (PET) with ^{15}O -water, ^{13}N -ammonia, and ^{82}Rb is the gold standard for assessing myocardial blood flow (MBF) and myocardial flow reserve (MFR) which are reliable indicators of the severity of coronary artery disease. Unfortunately, PET is not generally accessible because of exorbitant costs or the requirement of an on-site cyclotron (for ^{13}N -ammonia and ^{15}O -water) [11]. As a result, techniques based on single-photon emitting radiotracers were proposed as an alternative to PET. The viability of these approaches was demonstrated in several studies using dynamic planar and static SPECT methods [46–48]. Human studies showed that SPECT measurement of MBF and MFR using NaI-based general-purpose SPECT devices is possible [48–52]. Several articles were concentrated on the practicality of dynamic SPECT using CTZ detectors and the association of fractional flow reserve measurements with cardiac PET and invasive coronary angiography [11]. Several investigations have found that MBF and MFR measurements have acceptable intra- and inter-operator repeatability [53–58].

Patients with left main and three-vessel disease (3VD) had the highest risk of mortality due to CAD. The major purpose of noninvasive assessment is to detect this high-risk for whom

revascularization leads to improved symptoms and survival. Lima et al. [59] reported that adjunctive evaluation of function and perfusion by gated SPECT MPI improves identification of abnormalities in multiple vascular areas in patients with severe 3VD without reducing specificity.

It has been established that dynamic SPECT utilizing a CZT camera can help with coronary flow reserve (CFR) evaluation and characterization of high-risk coronary anatomy [60]. The use of dynamic imaging allows for the assessment of blood flow and CFR, which may be employed to diagnose the illness sooner and patients prevent misinterpreting three-vessel disease as normal [61]. Ben Bouallégue et al. [62] analyzed selected high-risk patients with multivessel diseases. They discovered that scintigraphic estimates of global and regional myocardial perfusion reserve in multivessel patients utilizing a CZT camera appear to correspond well with invasive angiographic results such as maximal stenosis and FFR values. According to current evidence, assessing MBF and MFR using a SPECT camera with CZT detectors is more appropriate than semi-quantitative MPI analysis and hence more precise in subjects with multivessel disease [11]. Several investigations utilizing FFR as the reference technique found a high level of concordance between FFR and a SPECT camera with CZT detectors measured MFR values, indicating that these two indices represent the same physiological processes [53, 55, 56, 62, 63]. However, unlike FFR, MFR is known to be affected by both conductive coronary artery stenosis and microvascular resistance [11]. MFR, as opposed to FFR, measures flow in the epicardial arteries and microvasculature. It should be emphasized that an abnormal MFR with a low FFR implies microvascular dysfunction or widespread CAD [3].

Miyagawa et al. [55] observed MFR index (K1 stress/K1 rest) values of 1.57 in the range of 1.45–1.68 for ^{99m}Tc -Tetrofosmin in 16 subjects and 1.61 in the range of 1.46–1.76 for ^{99m}Tc -MIBI in 17 subjects in low-risk of CAD patients. In patients with non-obstructive CAD, the global MFRi was 1.63 in the range of 1.22–2.04. Ben-Haim et al. [64] discovered comparable MFRi values of 1.58 (IQR 1.30–1.75) for the same patient subgroup. These findings are based on limited patient populations. In various studies, the estimates of the quantitative indexes varied between subjects with low-risk and non-obstructive coronary artery disease, indicating the need for more multicenter and multivendor research to establish normal values of CZT-SPECT-derived MBF and MFR [11].

Several researches have shown that regional MFR is reduced in left ventricle regions supplied by coronary arteries having more than 50% obstructive lesion [57, 62, 64]. Ben Bouallégue et al. [62] observed that for flow ratios with a threshold value of 2, regional MFR for diagnosing obstructive lesions had a sensitivity, specificity, and accuracy of 80%, 85%, and 81%, respectively. In diagnosing an obstructive lesion in the corresponding artery, De Souza et al. [57] found a regional MFR sensitivity of 63.2 % and specificity of 74.1 % with a cutoff of 2.2. In contrast, Nudi et al. [65] discovered no link between MFR and significant obstruction in coronary arteries in CAG.

The gold standard of anatomically diagnosed CAD is quantitative coronary angiography (QCA), which is frequently utilized for risk stratification. The occurrence of a link between QCA and CZT-SPECT is of important clinical relevance. It should be noted that this form of assessment does not entirely correspond to coronary physiology. Obstruction greater than 50% is not necessarily linked

with ischemia as shown by invasive FFR. These findings suggest that the appearance of normal MBF and MFR results in locations fed by coronary arteries with lesions of more than 50% does not always represent a false-negative result [11].

The link between regional and global MBF and MFR measurements and other factors, such as coronary artery burden indexes and obstruction severity, the existence of myocardial perfusion deficits, obtained using SPECT camera with CZT detectors and MBF estimated by positron emission tomography, have been studied. Nonetheless, standardization of acquisition and post-processing protocols, also software upgrades, are required to decrease inter-center variability and boost the clinical robustness of the SPECT camera with CZT outcomes [11].

Sympathetic innervation imaging

The link between measurements of regional myocardial adrenergic innervation heterogeneity, mechanical function, and also myocardial perfusion in subjects with CAD has been examined, utilizing a low-dose imaging protocol with a CZT-SPECT camera. A simultaneous assessment of myocardial perfusion and cardiac adrenergic innervations has been done with good image quality, short acquisition time, and a low radiation dose. When obtained using CZT-SPECT, measurements of adrenergic innervation heterogeneity were compared to standard planar indexes and improved the identification of individuals at increased cardiovascular risk by attaching meaningful regional data on myocardial adrenergic nerve activity [66].

The majority of the research is based on pictures obtained with ordinary Anger cameras, with an energy window of $159\text{ keV} \pm 20\%$ and without attenuation correction. ^{123}I -mIBG imaging using a CZT solid-state camera enables shorter acquisition time and improved energy resolution, allowing for simultaneous capture of adrenergic and perfusion images [67].

CZT-SPECT acquisition in obese patients

Unfortunately, the development of CZT cameras, which have benefits over traditional SPECT devices, does not solve the problem of image quality deterioration caused by obesity [1]. The Discovery NM 530c camera is prone to artifacts in extremely obese individuals due to its limited field of view and pinhole collimation geometry [68, 69]. Fiechter et al. [68] analyzed 81 patients, including 61 obese subjects. In patients with a BMI greater than 40 kg/m^2 , image quality was nondiagnostic in 81% of cases, after implementation of CT-based attenuation correction in 55%, respectively. As a result, in the case of The Discovery NM 530c individuals with a BMI of 40 kg/m^2 or higher should be referred for MPI scanning with a standard SPECT camera [1, 68].

This problem does not exist with the D-SPECT camera, and in uncertain cases is generated by diaphragmatic artifacts. It is worth reemphasizing that D-SPECT allows for examinations in two positions: upright and supine [35].

Conclusions

Nuclear cardiac imaging methods continue to be of significant practical importance to cardiologists, thanks to rapid and continuing technological progress and expansion. In comparison to gold

standards used in clinical practice, CZT-SPECT MPI, especially with the dynamic acquisition has excellent diagnostic sensitivity and specificity for CAD diagnosis. While MPI has several advantages in the assessment of coronary artery disease, it does expose individuals to ionizing radiation. Adherence to radiation safety best practices varied greatly amongst laboratories, although the ability to employ CZT-SPECT devices in nuclear cardiology enabled a significant decrease in radiation dose without sacrificing accuracy. To conclude, CZT-SPECT offers good image quality, low radiation dose and quick imaging acquisition for a more effective workflow, resulting in better patient comfort and more imaging protocol flexibility.

Conflict of interest

None declared.

References

1. Acampa W, Buechel RR, Gimelli A. Low dose in nuclear cardiology: state of the art in the era of new cadmium-zinc-telluride cameras. *Eur Heart J Cardiovasc Imaging*. 2016; 17(6): 591–595, doi: [10.1093/ehjci/jew036](https://doi.org/10.1093/ehjci/jew036), indexed in Pubmed: [26985078](https://pubmed.ncbi.nlm.nih.gov/26985078/).
2. Knutti J, Wijns W, Saraste A, et al. ESC Scientific Document Group. 2019 ESC Guidelines for the diagnosis and management of chronic coronary syndromes. *Eur Heart J*. 2020; 41(3): 407–477, doi: [10.1093/eurheartj/ehz425](https://doi.org/10.1093/eurheartj/ehz425), indexed in Pubmed: [31504439](https://pubmed.ncbi.nlm.nih.gov/31504439/).
3. Panjer M, Dobrolinska M, Wagenaar NRL, et al. Diagnostic accuracy of dynamic CZT-SPECT in coronary artery disease. A systematic review and meta-analysis. *J Nucl Cardiol*. 2021 [Epub ahead of print], doi: [10.1007/s12350-021-02721-8](https://doi.org/10.1007/s12350-021-02721-8), indexed in Pubmed: [34350553](https://pubmed.ncbi.nlm.nih.gov/34350553/).
4. Herzog BA, Buechel RR, Katz R, et al. Nuclear myocardial perfusion imaging with a cadmium-zinc-telluride detector technique: optimized protocol for scan time reduction. *J Nucl Med*. 2010; 51(1): 46–51, doi: [10.2967/jnumed.109.065532](https://doi.org/10.2967/jnumed.109.065532), indexed in Pubmed: [20008999](https://pubmed.ncbi.nlm.nih.gov/20008999/).
5. Marcassa C, Bax JJ, Bengel F, et al. European Council of Nuclear Cardiology (ECNC), European Society of Cardiology Working Group 5 (Nuclear Cardiology and Cardiac CT), European Association of Nuclear Medicine Cardiovascular Committee. Clinical value, cost-effectiveness, and safety of myocardial perfusion scintigraphy: a position statement. *Eur Heart J*. 2008; 29(4): 557–563, doi: [10.1093/eurheartj/ehm607](https://doi.org/10.1093/eurheartj/ehm607), indexed in Pubmed: [18202253](https://pubmed.ncbi.nlm.nih.gov/18202253/).
6. Picano E, Vañó E, Rehani MM, et al. The appropriate and justified use of medical radiation in cardiovascular imaging: a position document of the ESC Associations of Cardiovascular Imaging, Percutaneous Cardiovascular Interventions and Electrophysiology. *Eur Heart J*. 2014; 35(10): 665–672, doi: [10.1093/eurheartj/ehz394](https://doi.org/10.1093/eurheartj/ehz394), indexed in Pubmed: [24401558](https://pubmed.ncbi.nlm.nih.gov/24401558/).
7. Borges-Neto S, Pagnanelli RA, Shaw LK, et al. Clinical results of a novel wide beam reconstruction method for shortening scan time of Tc-99m cardiac SPECT perfusion studies. *J Nucl Cardiol*. 2007; 14(4): 555–565, doi: [10.1016/j.nuclcard.2007.04.022](https://doi.org/10.1016/j.nuclcard.2007.04.022), indexed in Pubmed: [17679065](https://pubmed.ncbi.nlm.nih.gov/17679065/).
8. DePuey EG, Gadiraju R, Clark J, et al. Ordered subset expectation maximization and wide beam reconstruction “half-time” gated myocardial perfusion SPECT functional imaging: a comparison to “full-time” filtered backprojection. *J Nucl Cardiol*. 2008; 15(4): 547–563, doi: [10.1016/j.nuclcard.2008.02.035](https://doi.org/10.1016/j.nuclcard.2008.02.035), indexed in Pubmed: [18674723](https://pubmed.ncbi.nlm.nih.gov/18674723/).
9. Giorgetti A, Rossi M, Stanislao M, et al. Myoview Imaging Optimization Group. Feasibility and diagnostic accuracy of a gated SPECT early-imaging protocol: a multicenter study of the Myoview Imaging Optimization Group. *J Nucl Med*. 2007; 48(10): 1670–1675, doi: [10.2967/jnumed.106.039107](https://doi.org/10.2967/jnumed.106.039107), indexed in Pubmed: [17873126](https://pubmed.ncbi.nlm.nih.gov/17873126/).
10. Kapur A, Latus KA, Davies G, et al. A comparison of three radionuclide myocardial perfusion tracers in clinical practice: the ROBUST study. *Eur J Nucl Med Mol Imaging*. 2002; 29(12): 1608–1616, doi: [10.1007/s00259-002-0998-8](https://doi.org/10.1007/s00259-002-0998-8), indexed in Pubmed: [12458395](https://pubmed.ncbi.nlm.nih.gov/12458395/).
11. Zavadovsky KV, Mochula AV, Maltseva AN, et al. The current status of CZT SPECT myocardial blood flow and reserve assessment: Tips and tricks. *J Nucl Cardiol*. 2021 [Epub ahead of print], doi: [10.1007/s12350-021-02620-y](https://doi.org/10.1007/s12350-021-02620-y), indexed in Pubmed: [33939162](https://pubmed.ncbi.nlm.nih.gov/33939162/).
12. Kincl V, Drozdová A, Vašina J, et al. Cadmium-zinc-telluride SPECT scanners - New perspectives in nuclear cardiology. *Cor et Vasa*. 2015; 57(3): e214–e218, doi: [10.1016/j.crvasa.2015.01.001](https://doi.org/10.1016/j.crvasa.2015.01.001).
13. Ben-Haim S, Kennedy J, Keidar Z. Novel Cadmium Zinc Telluride Devices for Myocardial Perfusion Imaging-Technological Aspects and Clinical Applications. *Semin Nucl Med*. 2016; 46(4): 273–285, doi: [10.1053/j.sem-nuclmed.2016.01.002](https://doi.org/10.1053/j.sem-nuclmed.2016.01.002), indexed in Pubmed: [27237438](https://pubmed.ncbi.nlm.nih.gov/27237438/).
14. Imbert L, Poussier S, Franken PR, et al. Compared performance of high-sensitivity cameras dedicated to myocardial perfusion SPECT: a comprehensive analysis of phantom and human images. *J Nucl Med*. 2012; 53(12): 1897–1903, doi: [10.2967/jnumed.112.107417](https://doi.org/10.2967/jnumed.112.107417), indexed in Pubmed: [23139084](https://pubmed.ncbi.nlm.nih.gov/23139084/).
15. Hudson HM, Larkin RS. Accelerated image reconstruction using ordered subsets of projection data. *IEEE Trans Med Imaging*. 1994; 13(4): 601–609, doi: [10.1109/42.363108](https://doi.org/10.1109/42.363108), indexed in Pubmed: [18218538](https://pubmed.ncbi.nlm.nih.gov/18218538/).
16. Buechel RR, Herzog BA, Husmann L, et al. Ultrafast nuclear myocardial perfusion imaging on a new gamma camera with semiconductor detector technique: first clinical validation. *Eur J Nucl Med Mol Imaging*. 2010; 37(4): 773–778, doi: [10.1007/s00259-009-1375-7](https://doi.org/10.1007/s00259-009-1375-7), indexed in Pubmed: [20107783](https://pubmed.ncbi.nlm.nih.gov/20107783/).
17. Fiechter M, Ghadri JR, Kuest SM, et al. Nuclear myocardial perfusion imaging with a novel cadmium-zinc-telluride detector SPECT/CT device: first validation versus invasive coronary angiography. *Eur J Nucl Med Mol Imaging*. 2011; 38(11): 2025–2030, doi: [10.1007/s00259-011-1877-y](https://doi.org/10.1007/s00259-011-1877-y), indexed in Pubmed: [21761267](https://pubmed.ncbi.nlm.nih.gov/21761267/).
18. Gimelli A, Bottai M, Giorgetti A, et al. Comparison between ultrafast and standard single-photon emission CT in patients with coronary artery disease: a pilot study. *Circ Cardiovasc Imaging*. 2011; 4(1): 51–58, doi: [10.1161/CIRCIMAGING.110.957399](https://doi.org/10.1161/CIRCIMAGING.110.957399), indexed in Pubmed: [21068188](https://pubmed.ncbi.nlm.nih.gov/21068188/).
19. Verger A, Djaballah W, Fourquet N, et al. Comparison between stress myocardial perfusion SPECT recorded with cadmium-zinc-telluride and Anger cameras in various study protocols. *Eur J Nucl Med Mol Imaging*. 2013; 40(3): 331–340, doi: [10.1007/s00259-012-2292-8](https://doi.org/10.1007/s00259-012-2292-8), indexed in Pubmed: [23184308](https://pubmed.ncbi.nlm.nih.gov/23184308/).
20. Soman P, Einstein AJ. Biologic effects of radiation from cardiac imaging: New insights from proteomic and genomic analyses. *J Nucl Cardiol*. 2016; 23(4): 754–757, doi: [10.1007/s12350-016-0517-0](https://doi.org/10.1007/s12350-016-0517-0), indexed in Pubmed: [27151300](https://pubmed.ncbi.nlm.nih.gov/27151300/).
21. Gambhir SS, Berman DS, Ziffer J, et al. A novel high-sensitivity rapid-acquisition single-photon cardiac imaging camera. *J Nucl Med*. 2009; 50(4): 635–643, doi: [10.2967/jnumed.108.060020](https://doi.org/10.2967/jnumed.108.060020), indexed in Pubmed: [19339672](https://pubmed.ncbi.nlm.nih.gov/19339672/).
22. Esteves FP, Raggi P, Folks RD, et al. Novel solid-state-detector dedicated cardiac camera for fast myocardial perfusion imaging: multicenter comparison with standard dual detector cameras. *J Nucl Cardiol*. 2009; 16(6): 927–934, doi: [10.1007/s12350-009-9137-2](https://doi.org/10.1007/s12350-009-9137-2), indexed in Pubmed: [19688410](https://pubmed.ncbi.nlm.nih.gov/19688410/).
23. Berman DS, Kang X, Tamarappoo B, et al. Stress thallium-201/rest technetium-99m sequential dual isotope high-speed myocardial perfusion imaging. *JACC Cardiovasc Imaging*. 2009; 2(3): 273–282, doi: [10.1016/j.jcmg.2008.12.012](https://doi.org/10.1016/j.jcmg.2008.12.012), indexed in Pubmed: [19356571](https://pubmed.ncbi.nlm.nih.gov/19356571/).
24. Duvall WL, Croft LB, Godiwala T, et al. Reduced isotope dose with rapid SPECT MPI imaging: initial experience with a CZT SPECT camera. *J Nucl Cardiol*. 2010; 17(6): 1009–1014, doi: [10.1007/s12350-010-9215-5](https://doi.org/10.1007/s12350-010-9215-5), indexed in Pubmed: [21069489](https://pubmed.ncbi.nlm.nih.gov/21069489/).
25. Duvall WL, Croft LB, Ginsberg ES, et al. Reduced isotope dose and imaging time with a high-efficiency CZT SPECT camera. *J Nucl Cardiol*. 2011; 18(5): 847–857, doi: [10.1007/s12350-011-9379-7](https://doi.org/10.1007/s12350-011-9379-7), indexed in Pubmed: [21528422](https://pubmed.ncbi.nlm.nih.gov/21528422/).
26. Einstein AJ, Blankstein R, Andrews H, et al. Comparison of image quality, myocardial perfusion, and left ventricular function between standard imaging and single-injection ultra-low-dose imaging using a high-efficiency SPECT

- camera: the MILLISIEVERT study. *J Nucl Med.* 2014; 55(9): 1430–1437, doi: [10.2967/jnumed.114.138222](https://doi.org/10.2967/jnumed.114.138222), indexed in Pubmed: [24982439](https://pubmed.ncbi.nlm.nih.gov/24982439/).
27. Sharir T, Ben-Haim S, Merzon K, et al. High-Speed Myocardial Perfusion Imaging. *JACC: Cardiovascular Imaging.* 2008; 1(2): 156–163, doi: [10.1016/j.jcmg.2007.12.004](https://doi.org/10.1016/j.jcmg.2007.12.004), indexed in Pubmed: [19356422](https://pubmed.ncbi.nlm.nih.gov/19356422/).
 28. Cantoni V, Green R, Acampa W, et al. Diagnostic performance of myocardial perfusion imaging with conventional and CZT single-photon emission computed tomography in detecting coronary artery disease: A meta-analysis. *J Nucl Cardiol.* 2021; 28(2): 698–715, doi: [10.1007/s12350-019-01747-3](https://doi.org/10.1007/s12350-019-01747-3), indexed in Pubmed: [31089962](https://pubmed.ncbi.nlm.nih.gov/31089962/).
 29. Nudi F, Iskandrian AE, Schillaci O, et al. Diagnostic Accuracy of Myocardial Perfusion Imaging With CZT Technology: Systemic Review and Meta-Analysis of Comparison With Invasive Coronary Angiography. *JACC Cardiovasc Imaging.* 2017; 10(7): 787–794, doi: [10.1016/j.jcmg.2016.10.023](https://doi.org/10.1016/j.jcmg.2016.10.023), indexed in Pubmed: [28330657](https://pubmed.ncbi.nlm.nih.gov/28330657/).
 30. Zhang YQ, Jiang YF, Hong Lu, et al. Diagnostic value of cadmium-zinc-telluride myocardial perfusion imaging versus coronary angiography in coronary artery disease: A PRISMA-compliant meta-analysis. *Medicine (Baltimore).* 2019; 98(9): e14716, doi: [10.1097/MD.00000000000014716](https://doi.org/10.1097/MD.00000000000014716), indexed in Pubmed: [30817614](https://pubmed.ncbi.nlm.nih.gov/30817614/).
 31. Gimelli A, Liga R, Duce V, et al. Accuracy of myocardial perfusion imaging in detecting multivessel coronary artery disease: A cardiac CZT study. *J Nucl Cardiol.* 2017; 24(2): 687–695, doi: [10.1007/s12350-015-0360-8](https://doi.org/10.1007/s12350-015-0360-8), indexed in Pubmed: [26846367](https://pubmed.ncbi.nlm.nih.gov/26846367/).
 32. Esteves FP, Galt JR, Folks RD, et al. Diagnostic performance of low-dose rest/stress Tc-99m tetrofosmin myocardial perfusion SPECT using the 530c CZT camera: quantitative vs visual analysis. *J Nucl Cardiol.* 2014; 21(1): 158–165, doi: [10.1007/s12350-013-9827-7](https://doi.org/10.1007/s12350-013-9827-7), indexed in Pubmed: [24287713](https://pubmed.ncbi.nlm.nih.gov/24287713/).
 33. Mirshahvalad SA, Chavoshi M, Hekmat S. Diagnostic performance of prone-only myocardial perfusion imaging versus coronary angiography in the detection of coronary artery disease: A systematic review and meta-analysis. *J Nucl Cardiol.* 2022; 29(3): 1339–1351, doi: [10.1007/s12350-020-02376-x](https://doi.org/10.1007/s12350-020-02376-x), indexed in Pubmed: [33025477](https://pubmed.ncbi.nlm.nih.gov/33025477/).
 34. Nishiyama Y, Miyagawa M, Kawaguchi N, et al. Combined supine and prone myocardial perfusion single-photon emission computed tomography with a cadmium zinc telluride camera for detection of coronary artery disease. *Circ J.* 2014; 78(5): 1169–1175, doi: [10.1253/circj.13-1316](https://doi.org/10.1253/circj.13-1316), indexed in Pubmed: [24572492](https://pubmed.ncbi.nlm.nih.gov/24572492/).
 35. Nakazato R, Tamarappoo BK, Kang X, et al. Quantitative upright-supine high-speed SPECT myocardial perfusion imaging for detection of coronary artery disease: correlation with invasive coronary angiography. *J Nucl Med.* 2010; 51(11): 1724–1731, doi: [10.2967/jnumed.110.078782](https://doi.org/10.2967/jnumed.110.078782), indexed in Pubmed: [20956478](https://pubmed.ncbi.nlm.nih.gov/20956478/).
 36. Perrin M, Roch V, Claudin M, et al. Assessment of Myocardial CZT SPECT Recording in a Forward-Leaning Bikerlike Position. *J Nucl Med.* 2019; 60(6): 824–829, doi: [10.2967/jnumed.118.217695](https://doi.org/10.2967/jnumed.118.217695), indexed in Pubmed: [30389818](https://pubmed.ncbi.nlm.nih.gov/30389818/).
 37. Abidov A, Germano G, Hachamovitch R, et al. Gated SPECT in assessment of regional and global left ventricular function: major tool of modern nuclear imaging. *J Nucl Cardiol.* 2006; 13(2): 261–279, doi: [10.1007/BF02971251](https://doi.org/10.1007/BF02971251), indexed in Pubmed: [16580963](https://pubmed.ncbi.nlm.nih.gov/16580963/).
 38. Cochet H, Bullier E, Gerbaud E, et al. Absolute quantification of left ventricular global and regional function at nuclear MPI using ultrafast CZT SPECT: initial validation versus cardiac MR. *J Nucl Med.* 2013; 54(4): 556–563, doi: [10.2967/jnumed.112.110577](https://doi.org/10.2967/jnumed.112.110577), indexed in Pubmed: [23385955](https://pubmed.ncbi.nlm.nih.gov/23385955/).
 39. Giorgetti A, Masci PG, Marras G, et al. Gated SPECT evaluation of left ventricular function using a CZT camera and a fast low-dose clinical protocol: comparison to cardiac magnetic resonance imaging. *Eur J Nucl Med Mol Imaging.* 2013; 40(12): 1869–1875, doi: [10.1007/s00259-013-2505-9](https://doi.org/10.1007/s00259-013-2505-9), indexed in Pubmed: [23884280](https://pubmed.ncbi.nlm.nih.gov/23884280/).
 40. Claudin M, Imbert L, Djabballah W, et al. Routine evaluation of left ventricular function using CZT-SPECT, with low injected activities and limited recording times. *J Nucl Cardiol.* 2018; 25(1): 249–256, doi: [10.1007/s12350-016-0615-z](https://doi.org/10.1007/s12350-016-0615-z), indexed in Pubmed: [27677613](https://pubmed.ncbi.nlm.nih.gov/27677613/).
 41. Sala M, Kincl V, Kamínek M, et al. Assessment of left ventricular volumes and ejection fraction using ultra-low-dose thallium-201 SPECT on a CZT camera: a comparison with magnetic resonance imaging. *J Nucl Cardiol.* 2022; 29(1): 181–187, doi: [10.1007/s12350-020-02161-w](https://doi.org/10.1007/s12350-020-02161-w), indexed in Pubmed: [32410056](https://pubmed.ncbi.nlm.nih.gov/32410056/).
 42. Bailliez A, Blaire T, Mouquet F, et al. Segmental and global left ventricular function assessment using gated SPECT with a semiconductor Cadmium Zinc Telluride (CZT) camera: phantom study and clinical validation vs cardiac magnetic resonance. *J Nucl Cardiol.* 2014; 21(4): 712–722, doi: [10.1007/s12350-014-9899-z](https://doi.org/10.1007/s12350-014-9899-z), indexed in Pubmed: [24810429](https://pubmed.ncbi.nlm.nih.gov/24810429/).
 43. Coupez E, Merlin C, Tuyisenge V, et al. Validation of cadmium-zinc-telluride camera for measurement of left ventricular systolic performance. *J Nucl Cardiol.* 2018; 25(3): 1029–1036, doi: [10.1007/s12350-017-0816-0](https://doi.org/10.1007/s12350-017-0816-0), indexed in Pubmed: [28194726](https://pubmed.ncbi.nlm.nih.gov/28194726/).
 44. Gimelli A, Liga R, Pasanisi EM, et al. Evaluation of left ventricular diastolic function with a dedicated cadmium-zinc-telluride cardiac camera: comparison with Doppler echocardiography. *Eur Heart J Cardiovasc Imaging.* 2014; 15(9): 972–979, doi: [10.1093/ehjci/jeu037](https://doi.org/10.1093/ehjci/jeu037), indexed in Pubmed: [24618658](https://pubmed.ncbi.nlm.nih.gov/24618658/).
 45. Gimelli A, Liga R, Bottai M, et al. Diastolic dysfunction assessed by ultra-fast cadmium-zinc-telluride cardiac imaging: impact on the evaluation of ischaemia. *Eur Heart J Cardiovasc Imaging.* 2015; 16(1): 68–73, doi: [10.1093/ehjci/jeu166](https://doi.org/10.1093/ehjci/jeu166), indexed in Pubmed: [25187611](https://pubmed.ncbi.nlm.nih.gov/25187611/).
 46. Gullberg GT, Di Bella EV, Sinusas AJ. Estimation of coronary flow reserve: can SPECT compete with other modalities? *J Nucl Cardiol.* 2001; 8(5): 620–625, doi: [10.1067/mnc.2001.118121](https://doi.org/10.1067/mnc.2001.118121), indexed in Pubmed: [11593228](https://pubmed.ncbi.nlm.nih.gov/11593228/).
 47. Iida H, Eberl S, Kim KM, et al. Absolute quantitation of myocardial blood flow with (201)Tl and dynamic SPECT in canine: optimisation and validation of kinetic modelling. *Eur J Nucl Med Mol Imaging.* 2008; 35(5): 896–905, doi: [10.1007/s00259-007-0654-4](https://doi.org/10.1007/s00259-007-0654-4), indexed in Pubmed: [18202845](https://pubmed.ncbi.nlm.nih.gov/18202845/).
 48. Hsu B, Hu LH, Yang BH, et al. SPECT myocardial blood flow quantitation toward clinical use: a comparative study with N-Ammonia PET myocardial blood flow quantitation. *Eur J Nucl Med Mol Imaging.* 2017; 44(1): 117–128, doi: [10.1007/s00259-016-3491-5](https://doi.org/10.1007/s00259-016-3491-5), indexed in Pubmed: [27585576](https://pubmed.ncbi.nlm.nih.gov/27585576/).
 49. Sugihara H, Yonekura Y, Kataoka K, et al. Estimation of coronary flow reserve with the use of dynamic planar and SPECT images of Tc-99m tetrofosmin. *J Nucl Cardiol.* 2001; 8(5): 575–579, doi: [10.1067/mnc.2001.115934](https://doi.org/10.1067/mnc.2001.115934), indexed in Pubmed: [11593222](https://pubmed.ncbi.nlm.nih.gov/11593222/).
 50. Klein R, Hung GU, Wu TC, et al. Feasibility and operator variability of myocardial blood flow and reserve measurements with ¹¹¹mTc-sestamibi quantitative dynamic SPECT/CT imaging. *J Nucl Cardiol.* 2014; 21(6): 1075–1088, doi: [10.1007/s12350-014-9971-8](https://doi.org/10.1007/s12350-014-9971-8), indexed in Pubmed: [25280761](https://pubmed.ncbi.nlm.nih.gov/25280761/).
 51. Winant CD, Aparici CM, Zelnik YR, et al. Investigation of dynamic SPECT measurements of the arterial input function in human subjects using simulation, phantom and human studies. *Phys Med Biol.* 2012; 57(2): 375–393, doi: [10.1088/0031-9155/57/2/375](https://doi.org/10.1088/0031-9155/57/2/375), indexed in Pubmed: [22170801](https://pubmed.ncbi.nlm.nih.gov/22170801/).
 52. Shrestha U, Sciammarella M, Alhassen F, et al. Measurement of absolute myocardial blood flow in humans using dynamic cardiac SPECT and Tc-tetrofosmin: Method and validation. *J Nucl Cardiol.* 2017; 24(1): 268–277, doi: [10.1007/s12350-015-0320-3](https://doi.org/10.1007/s12350-015-0320-3), indexed in Pubmed: [26715603](https://pubmed.ncbi.nlm.nih.gov/26715603/).
 53. Agostini D, Roule V, Nganoa C, et al. First validation of myocardial flow reserve assessed by dynamic Tc-sestamibi CZT-SPECT camera: head to head comparison with O-water PET and fractional flow reserve in patients with suspected coronary artery disease. The WATERDAY study. *Eur J Nucl Med Mol Imaging.* 2018; 45(7): 1079–1090, doi: [10.1007/s00259-018-3958-7](https://doi.org/10.1007/s00259-018-3958-7), indexed in Pubmed: [29497801](https://pubmed.ncbi.nlm.nih.gov/29497801/).
 54. Otaki Y, Manabe O, Miller RJH, et al. Quantification of myocardial blood flow by CZT-SPECT with motion correction and comparison with O-water PET. *J Nucl Cardiol.* 2021; 28(4): 1477–1486, doi: [10.1007/s12350-019-01854-1](https://doi.org/10.1007/s12350-019-01854-1), indexed in Pubmed: [31452085](https://pubmed.ncbi.nlm.nih.gov/31452085/).
 55. Miyagawa M, Nishiyama Y, Uetani T, et al. Estimation of myocardial flow reserve utilizing an ultrafast cardiac SPECT: Comparison with coronary angiography, fractional flow reserve, and the SYNTAX score. *Int J Cardiol.* 2017; 244: 347–353, doi: [10.1016/j.ijcard.2017.06.012](https://doi.org/10.1016/j.ijcard.2017.06.012), indexed in Pubmed: [28622946](https://pubmed.ncbi.nlm.nih.gov/28622946/).

56. Han S, Kim YH, Ahn JM, et al. Feasibility of dynamic stress TI/rest Tc-tetrofosmin single photon emission computed tomography for quantification of myocardial perfusion reserve in patients with stable coronary artery disease. *Eur J Nucl Med Mol Imaging*. 2018; 45(12): 2173–2180, doi: [10.1007/s00259-018-4057-5](https://doi.org/10.1007/s00259-018-4057-5), indexed in Pubmed: [29858614](https://pubmed.ncbi.nlm.nih.gov/29858614/).
57. de Souza AC, Gonçalves BKD, Tedeschi AL, et al. Quantification of myocardial flow reserve using a gamma camera with solid-state cadmium-zinc-telluride detectors: Relation to angiographic coronary artery disease. *J Nucl Cardiol*. 2021; 28(3): 876–884, doi: [10.1007/s12350-019-01775-z](https://doi.org/10.1007/s12350-019-01775-z), indexed in Pubmed: [31222529](https://pubmed.ncbi.nlm.nih.gov/31222529/).
58. Wells RG, Radonjic I, Clackdoyle D, et al. Test-Retest Precision of Myocardial Blood Flow Measurements With Tc-Tetrofosmin and Solid-State Detector Single Photon Emission Computed Tomography. *Circ Cardiovasc Imaging*. 2020; 13(2): e009769, doi: [10.1161/CIRCIMAGING.119.009769](https://doi.org/10.1161/CIRCIMAGING.119.009769), indexed in Pubmed: [32069116](https://pubmed.ncbi.nlm.nih.gov/32069116/).
59. Lima R, Watson D, Goode A, et al. Incremental value of combined perfusion and function over perfusion alone by gated SPECT myocardial perfusion imaging for detection of severe three-vessel coronary artery disease. *J Am Coll Cardiol*. 2003; 42(1): 64–70, doi: [10.1016/s0735-1097\(03\)00562-x](https://doi.org/10.1016/s0735-1097(03)00562-x), indexed in Pubmed: [12849661](https://pubmed.ncbi.nlm.nih.gov/12849661/).
60. Slomka PJ, Berman DS, Germano G. Absolute myocardial blood flow quantification with SPECT/CT: is it possible? *J Nucl Cardiol*. 2014; 21(6): 1092–1095, doi: [10.1007/s12350-014-0002-6](https://doi.org/10.1007/s12350-014-0002-6), indexed in Pubmed: [25294433](https://pubmed.ncbi.nlm.nih.gov/25294433/).
61. Shiraishi S, Sakamoto F, Tsuda N, et al. Prediction of left main or 3-vessel disease using myocardial perfusion reserve on dynamic thallium-201 single-photon emission computed tomography with a semiconductor gamma camera. *Circ J*. 2015; 79(3): 623–631, doi: [10.1253/circj.CJ-14-0932](https://doi.org/10.1253/circj.CJ-14-0932), indexed in Pubmed: [25746547](https://pubmed.ncbi.nlm.nih.gov/25746547/).
62. Ben Bouallègue F, Roubille F, Lattuca B, et al. SPECT Myocardial Perfusion Reserve in Patients with Multivessel Coronary Disease: Correlation with Angiographic Findings and Invasive Fractional Flow Reserve Measurements. *J Nucl Med*. 2015; 56(11): 1712–1717, doi: [10.2967/jnumed.114.143164](https://doi.org/10.2967/jnumed.114.143164), indexed in Pubmed: [26338893](https://pubmed.ncbi.nlm.nih.gov/26338893/).
63. Zavadovsky KV, Mochula AV, Boshchenko AA, et al. Absolute myocardial blood flows derived by dynamic CZT scan vs invasive fractional flow reserve: Correlation and accuracy. *J Nucl Cardiol*. 2021; 28(1): 249–259, doi: [10.1007/s12350-019-01678-z](https://doi.org/10.1007/s12350-019-01678-z), indexed in Pubmed: [30847856](https://pubmed.ncbi.nlm.nih.gov/30847856/).
64. Ben-Haim S, Murthy VL, Breault C, et al. Quantification of Myocardial Perfusion Reserve Using Dynamic SPECT Imaging in Humans: A Feasibility Study. *J Nucl Med*. 2013; 54(6): 873–879, doi: [10.2967/jnumed.112.109652](https://doi.org/10.2967/jnumed.112.109652), indexed in Pubmed: [23578996](https://pubmed.ncbi.nlm.nih.gov/23578996/).
65. Nudi F, Biondi-Zoccai G, Nudi A, et al. Comparative analysis between myocardial perfusion reserve and maximal ischemia score at single photon emission computed tomography with new-generation cadmium-zinc-telluride cameras. *J Nucl Cardiol*. 2021; 28(3): 1072–1084, doi: [10.1007/s12350-019-01764-2](https://doi.org/10.1007/s12350-019-01764-2), indexed in Pubmed: [31152316](https://pubmed.ncbi.nlm.nih.gov/31152316/).
66. Gimelli A, Liga R, Giorgetti A, et al. Assessment of myocardial adrenergic innervation with a solid-state dedicated cardiac cadmium-zinc-telluride camera: first clinical experience. *Eur Heart J Cardiovasc Imaging*. 2014; 15(5): 575–585, doi: [10.1093/ehjci/jet258](https://doi.org/10.1093/ehjci/jet258), indexed in Pubmed: [24351314](https://pubmed.ncbi.nlm.nih.gov/24351314/).
67. Wan N, Travin MI. Cardiac Imaging With I-meta-iodobenzylguanidine and Analogous PET Tracers: Current Status and Future Perspectives. *Semin Nucl Med*. 2020; 50(4): 331–348, doi: [10.1053/j.semnuclmed.2020.03.001](https://doi.org/10.1053/j.semnuclmed.2020.03.001), indexed in Pubmed: [32540030](https://pubmed.ncbi.nlm.nih.gov/32540030/).
68. Fiechter M, Gebhard C, Fuchs TA, et al. Cadmium-zinc-telluride myocardial perfusion imaging in obese patients. *J Nucl Med*. 2012; 53(9): 1401–1406, doi: [10.2967/jnumed.111.102434](https://doi.org/10.2967/jnumed.111.102434), indexed in Pubmed: [22870823](https://pubmed.ncbi.nlm.nih.gov/22870823/).
69. Budzyńska A, Osiecki S, Mazurek A, et al. Feasibility of myocardial perfusion imaging studies in morbidly obese patients with a cadmium-zinc-telluride cardiac camera. *Nucl Med Rev Cent East Eur*. 2019; 22(1): 18–22, doi: [10.5603/NMR.2019.0003](https://doi.org/10.5603/NMR.2019.0003), indexed in Pubmed: [31482538](https://pubmed.ncbi.nlm.nih.gov/31482538/).